



Short Communication

Cavitation-induced radical-chain oxidation of valeric aldehyde

Ulrich Neuenschwander^a, Jürg Neuenschwander^b, Ive Hermans^{a,*}^a Department of Chemistry and Applied Biosciences, ETH Zurich, 8093 Zurich, Switzerland^b Empa, Swiss Federal Laboratories for Materials Science and Technology, 8600 Dübendorf, Switzerland

ARTICLE INFO

Article history:

Received 13 December 2011

Received in revised form 2 February 2012

Accepted 6 February 2012

Available online 15 February 2012

Keywords:

Cavitation

Oxidation

Radicals

Peroxide

ABSTRACT

The application of high-amplitude ultrasound to liquids triggers cavitation. By the collapse of the thereby appearing vacuum cavities, high temperatures can be reached in a transient manner. The high temperatures in these hot-spots can lead to homolytic scission of chemical bonds. The thereby generated radicals are usually utilized in aqueous systems for the degeneration of organic pollutants. In this contribution, we demonstrate that the radicals can also be used for synthetic purposes: under an oxygen atmosphere, they trigger the oxidation of an aldehyde substrate.

© 2012 Elsevier B.V. All rights reserved.

1. Introduction

1.1. Chemical effects of ultrasound

The chemical effects of ultrasound can be mainly classified into two categories. The first category comprises heterogeneous reactions, where the ultrasound enforces a high-frequency mechanical mixing, leading to superior mass-transfer, when compared with classical agitation. Popular applications that fall into this category are dispersion of solids in liquids [1] and phase-transfer reactions using liquid–liquid emulsions [2,3]. A promising approach is for instance the compatibilization of aqueous oxidants with organic substrates [4]. Such heterogeneous reactions are established technology [5].

The second category comprises homogeneous reactions in liquids, where highly reactive radical intermediates are formed in a process called cavitation [6]. So far, the most important representatives of this second category are advanced oxidation processes (AOP's), where organic pollutants in waste-water are oxidatively degraded [7]. In principle, though, cavitation-generated radicals can also be used for synthetic purposes. A review about synthetic sonochemistry mentions the efforts that have been made so far [8]. The available examples are still rare, the most prominent being the sonolytic initiation of radical polymerization [9], the Ph_3SnH -based hydrostannation of alkenes [10], and the isomerizations of organic [11] or coordination compounds [12]. Since oxidations are often chain-propagated radical reactions (see below), a

sonochemical improvement of those reactions stands to reason. Indeed, in a preliminary observation, Chervinsky realized that the rate of cyclohexane oxidation was higher under intense ultrasonic treatment [13]. Moreover, a similar effect was observed in the oxidation of aldehydes [14]. As a step forward in the valorization of synthetic sonochemistry, we characterize in this paper the cavitation-induced oxidation of valeric aldehyde under solvent-free conditions.

1.2. Ultrasonic cavitation

The chemical and physical processes that are associated with the cavitation phenomenon have been characterized in the literature: Due to the negative pressure, induced by the fast movement of an ultrasound-transmitter, vacuum bubbles are formed in the liquid phase [6a]. These bubbles have a certain lifetime, yet they collapse and provoke the formation of a hot-spot in the liquid, with temperatures locally reaching very high values [15]. The appearance of such cavities – not necessarily their efficiency – is basically frequency-independent and even occurs at very short sonication pulses [16]. The apparent heating and cooling rates is exorbitantly high, and steep temperature gradients, far from equilibrium, appear [17]. With this, very peculiar reaction conditions can be achieved, albeit operating the reactor at room temperature and ambient pressure.

If components of low boiling-point are present, they tend to diffuse into the vacuum bubble and lower the intensity of the collapse (“buffer” effect), leading to a lower peak temperature [18]. Therefore, the cavitation is more pronounced at low temperatures and the use of low-boiling solvents is to be avoided for high cavitation

* Corresponding author.

E-mail address: hermans@chem.ethz.ch (I. Hermans).

efficiencies [19]. Due to the high peak temperatures reached in the hot-spot, even chemical (covalent) bonds can be broken. If the bond-breaking happens homolytically, the formation of radical species (i.e. molecules with an unpaired electron) can be observed [20].

1.3. Autoxidation

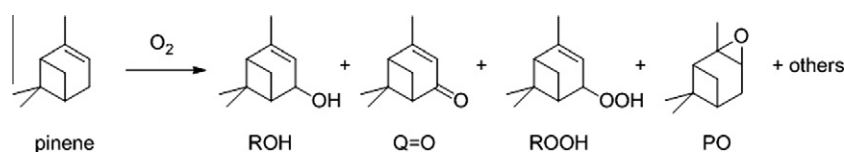
The selective oxidation of hydrocarbon substrates using oxygen as oxidant – sometimes referred to as *autoxidation* – is both an industrially relevant and intellectually challenging task [21]. Having access to a wide range of process parameters can be beneficial for the optimization of the product selectivity. Since oxygen has a paramagnetic ground state (i.e. triplet O_2), these oxidations rely on the occurrence of other open-shell species, e.g. radicals, derived from the substrate [22]. It is known that by the presence of peroxides, a finite quasi-constant radical concentration – necessary to maintain the oxidation – can be achieved. This is because of the (relatively) weak O–O bond of about 40 kcal mol^{-1} , that can be thermally activated at elevated temperatures [23]. Particularly for that reason, radical chain oxidations at room temperature are a challenge.

A general oxidation mechanism [23b] can be summarized as follows: Upon unimolecular initiation of a dialkylperoxide (ROOR) molecule (reaction 1a) or bimolecular initiation (reaction 1b) of a hydroperoxide (ROOH) molecule with a substrate molecule (RH), alkoxy (RO \cdot) and alkyl (R \cdot) radicals are formed. The alkyl radical adds in a very fast step an oxygen molecule (reaction 2) to form a peroxy radical (ROO \cdot). Both, alkoxy and peroxy radicals, can abstract a hydrogen atom from the substrate (reactions 3–4), thereby regenerating an alkyl radical. Like this, many product molecules are formed with oxygen as the terminal oxidant. A radical runaway is prevented by mutual reaction of peroxy radicals, leading to termination (reaction 5), forming non-radical alcohol (ROH) and carbonyl (Q=O) compounds. Under conditions where the propagation is much faster than the termination (i.e. a high chain length), the vast majority of the products arises from propagation steps. The most abundant radicals in the system (pure hydrocarbon solution; [RH] = 6–9 M) are peroxy radicals (ROO \cdot ; approx. 10^{-7} M), due to their – relatively – low reactivity.

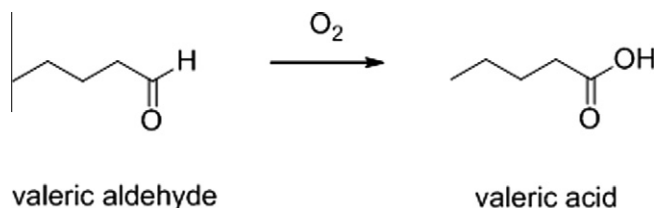


Scheme 1 shows an example of such an autoxidation reaction, using the alkene substrate α -pinene [24]. In that case, most of the obtained products are interesting targets for the flavour and fragrance industry, e.g. the epoxide is the starting material for the synthesis of sandalore (Givaudan) and polysantol (Firmenich) [25].

The overall oxidation rate is mostly governed by the substrate's C–H bond dissociation energy and the reactivity of the peroxy radical. For instance, alkenes react faster than alkanes, because of their



Scheme 1. Main products of the thermal α -pinene autoxidation at 353 K: Alcohol (ROH), ketone (Q = O), hydroperoxide (ROOH) and epoxide (PO).



Scheme 2. Thermal autoxidation of valeric aldehyde.

weaker α -C–H bond. Aldehydes react faster than alkenes for the same reason. Moreover, the peroxy radicals formed in aldehyde autoxidation are particularly reactive [26] and thus, the propagation of the radical chain is significantly favoured. As an example, the aerobic oxidation of valeric aldehyde (*n*-pentanal) leads to the formation of valeric acid (*n*-pentanoic acid), as depicted in Scheme 2. The scale of this important chemical process is about 2×10^4 t/a worldwide [27]. The main applications of valeric acid are lubricants, PVC stabilizers and fragrances.

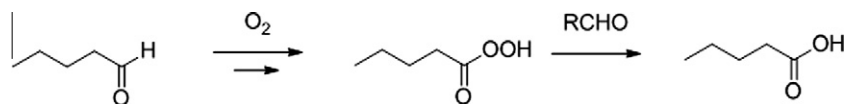
The accepted mechanism of such aerobic aldehyde oxidations involves a two-step process [28]. First, the aldehyde is oxidized to a peracid, which then in a second step undergoes a heterolytic Bayer–Villiger type oxidation of the substrate, yielding two equivalents of acid (Scheme 3). When using potassium salts as additives, an increased selectivity can be obtained, possibly by suppressing molecular rearrangements leading to formate esters [29].

2. Material and methods

The catalytic oxidation experiments were carried out in a home-made, water-cooled batch reactor with 20 mL capacity, filled up to 10 mL. Sonification was done with a Hielscher UP50H processor, working at 30 kHz, equipped with a 2 mm diameter sonotrode. The ultrasonic processor worked at 13 W, the amplitude was 220 μm and the acoustic efficiency 30%, measured calorimetrically. The reactions were operated at room temperature and ambient pressure. An immersed spiral water cooling system ensured a constant reaction temperature of 25 ± 3 °C. Valeric aldehyde (Acros, 97%) was chosen as model substrate due to its low vapour pressure (26 hPa at 20 °C, i.e. similar to water), facilitating ultrasonic cavitation. Pure oxygen (5.0, PanGas) was continuously bubbled through the reactor at 30 mL min^{-1} , and 1 mol% of di-*tert*-butyl peroxide (Merck, 96%) was added for the cavitation-induced formation of radicals. Quantitative analysis of the reaction mixture was done with gas chromatography (decane as internal standard, FID-detector, HP-5 column; starting temperature: 70 °C, ramp rate: 3° min^{-1} to 200 °C), by comparison with genuine product samples. To ensure that traces of peracid were included in the measurement, the samples were reduced with trimethylphosphine (Aldrich, 1 M in toluene).

3. Results and discussion

Typically, a chemical bond such as C–H has a bond dissociation energy (BDE) of $>80 \text{ kcal mol}^{-1}$. For calculating approximate



Scheme 3. Mechanism of thermal aldehyde autoxidation.

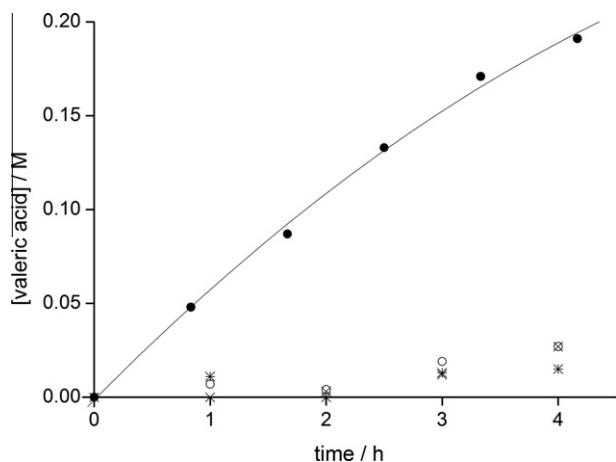


Fig. 1. Cavitation-induced autoxidation of valeric aldehyde, leading to valeric acid, under standard conditions (●). Under either N₂ flow (×), without ultrasound (○), or in the presence of 1 mol% BHT (*), the reaction hardly proceeds.

rate constants of elementary reactions, one can apply transition state theory (TST) [30]. Using a prefactor of 10^{15} s^{-1} , the TST rate constant for homolytic C–H dissociation becomes $3 \times 10^{-3} \text{ s}^{-1}$ at an estimated cavitation peak temperature of 1000 K. Thus, it is difficult to quantitatively functionalize this bond by direct sonolysis. However, the weaker the chemical bonds, the more pronounced the bond-breaking effect. Indeed, it has been reported that upon addition of carbon tetrachloride (C–Cl BDE 80 kcal mol⁻¹) to water (O–H BDE 120 kcal mol⁻¹) the efficiency of an ultrasonic AOP for micropurification could be increased significantly [31]. Our approach is similar: To strive for an indirect C–H sonolysis, by adding peroxides to the mixture, taking advantage of the sonolytically labile O–O peroxide bond (BDE 40 kcal mol⁻¹) that can be cleaved in the hot-spot and release radicals to the bulk. Our hypothesis is that these radicals can subsequently attack the C–H bonds of aldehyde molecules in a chain-reaction in the bulk. As a promising prerequisite, the low O–O BDE gives rise to a TST rate constant – under the same conditions as above – of $2 \times 10^6 \text{ s}^{-1}$, i.e. nine orders of magnitude faster as compared to sonolysis of C–H bonds.

Preliminary experiments revealed that at room temperature, the cavitation-induced oxidation of alkenes did not lead to significant accumulation of products. Therefore, we focused on the oxidation of aldehydes, where the intermediate peroxy radicals are much more reactive, because they possess an electron-withdrawing group in α -position (so-called acyl peroxy radicals). Fig. 1 shows the cavitation-induced autoxidation of valeric aldehyde (RCHO) to valeric acid (RCOOH).

Valeric acid was the predominant product and phosphine reduction of the sample did not lead to a bigger peak area in the chromatogram. Therefore, percarboxylic acid was present in the product mixture only to a negligible extent. However, about 10% side-products were observed at slightly lower retention times. Moreover, if the ultrasound was disconnected, or if O₂ flow was exchanged by N₂ flow, hardly any product was formed (Fig. 1). And in agreement with the radical character of the reaction, barely any product was formed when the radical scavenger 2,6-di-*tert*-butyl para-cresol (BHT) [32] was added.

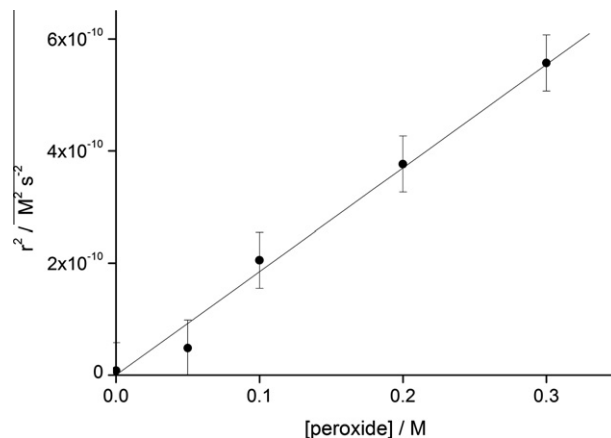


Fig. 2. Effect of the initially added di-*tert*-butyl peroxide concentration on the square of the apparent rate of cavitation-induced autoxidation of valeric aldehyde. The slope of the observed line is defined as α .

We also studied the oxidation rate r (i.e. time-derivative of valeric acid concentration in Fig. 1, as determined during the first hour reaction time) as a function of the peroxide concentration. As a matter of fact, radical chain reactions are kinetically characterized by a linear relationship between the squared-rate and the concentration of the species responsible for initiation [33]. Indeed, when plotting the kinetic data in such a squared-rate graph, a straight line was obtained (Fig. 2), confirming, our hypothesis of cavitation-induced initiation of the radical-chain oxidation. Moreover, from the slope of the line ($\alpha = 1.8 \times 10^{-9} \text{ M}^{-3} \text{ s}^{-2}$), information about the cavitation process can be obtained.

In the following part, we elaborate on the theoretical basis of the kinetics behind this process. According to our hypothesis, the chain initiation, i.e. the formation of radicals, can only occur in the liquid-phase hot-spots. Therefore it is convenient to define the ratio of the hot-spot volume to the total volume as f (Eq. (A)).

$$f \equiv \frac{V_{\text{hot-spot}}}{V_{\text{total}}} \quad (\text{A})$$

Under these assumptions, the kinetic equation for the overall reaction rate (Eq. (B)) can be adapted to yield a non-equilibrium form (Eq. (C))

$$r_{\text{eff}} = k_{\text{prop}} \cdot [\text{RCHO}] \cdot [\text{ROO}] \quad (\text{B})$$

$$r_{\text{eff}} = k_{\text{prop}}(298 \text{ K}) \cdot [\text{RCHO}] \cdot \sqrt{\frac{f \cdot k_{\text{init}}(T_{\text{hot-spot}}) \cdot [\text{ROOR}]}{k_{\text{term}}(298 \text{ K})}} \quad (\text{C})$$

In our experiment, we can determine α (see above), and by comparison of coefficients one gets Eq. (D)

$$\alpha = \frac{\partial(r_{\text{eff}})^2}{\partial[\text{ROOR}]} = \frac{k_{\text{prop}}(298 \text{ K})^2 \cdot [\text{RCHO}]^2 \cdot f \cdot k_{\text{init}}(T_{\text{hot-spot}})}{k_{\text{term}}(298 \text{ K})} \quad (\text{D})$$

Based on this, one can calculate the product of f and $k_{\text{init}}(T)$ (Eq. (E)) by using literature data for the other parameters: $k_{\text{term}}(298 \text{ K}) = 10^8 \text{ M}^{-1} \text{ s}^{-1}$, $k_{\text{prop}}(298 \text{ K}) = 7 \times 10^3 \text{ M}^{-1} \text{ s}^{-1}$ ($3 \times 10^3 \text{ M}^{-1} \text{ s}^{-1}$ at 273 K, extrapolated to 298 K with a temperature dependency of 7 kcal mol⁻¹ [34]) and $[\text{RCHO}] = 9.4 \text{ M}$

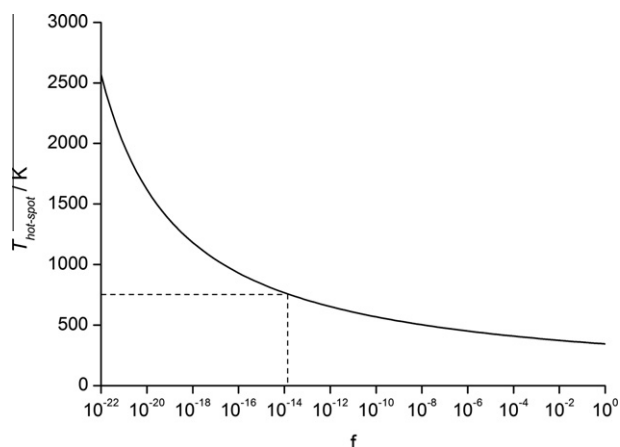


Fig. 3. The hot-spot temperature as a function of the hot-spot volume fraction f . The dashed line indicates the approximate situation for Misik's hot-spot temperature [35].

$$f \cdot k_{\text{init}}(T_{\text{hot-spot}}) = \frac{\alpha \cdot k_{\text{term}}(298 \text{ K})}{k_{\text{prop}}(268 \text{ K})^2 \cdot [\text{RCHO}]^2} = 4 \times 10^{-11} \text{ s}^{-1} \quad (\text{E})$$

Next, by introduction of a TST prefactor of 10^{15} s^{-1} and an activation energy of 40 kcal mol^{-1} for $k_{\text{init}}(T)$ [35], the f -dependency of $T_{\text{hot-spot}}$ can be calculated (Eq. (F) and Fig. 3)

$$\frac{T_{\text{hot-spot}}}{\text{K}} = \frac{20128}{\ln(f) + 58.48} \quad (\text{F})$$

Using Misik's experimental value of the hot-spot temperature in alkanes [36], i.e. 750 K , the estimation of f becomes 10^{-14} (see Fig. 3). Hence, the collapsed hot-spot volume in our 10 mL reactor is only about $1 \mu\text{m}^3$. Note that, albeit the relative volume fraction is known, the number and size of hot-spots cannot be derived from the available data. In principle, a high number of hot-spots with extremely small volumes, down to the nm^3 range is possible. Indeed, when applying a literature value of 10^{13} hot-spots per cubic meter [14], the average diameter is calculated to be around 1 nm . Although this is a microscopic volume, the chain initiation that happens in these hot-spots does have macroscopic implications, by enabling chain propagation in the bulk volume.

At a typical experiment with $[\text{ROOH}] = 0.1 \text{ M}$, an overall rate of $4 \times 10^{-5} \text{ M s}^{-1}$ can be observed. Using Eq. (B), a quasi-constant radical concentration in the bulk of $6 \times 10^{-10} \text{ M}$ can be calculated. Thus, the total termination rate equals $4 \times 10^{-11} \text{ M s}^{-1}$ and the chain length is approximately 10^6 . This supports our hypothesis of a chain oxidation process. This chain length is substantial and in agreement with values established in bromine-assisted sonoisomerization of alkenes [11], i.e. 10^4 .

4. Conclusions

In this contribution, we characterize radical-chain oxidations that are initiated by ultrasonic cavitation. Working at room temperature, the substrate valeric aldehyde was successfully oxidized with oxygen to valeric acid. A dialkyl peroxide was used as sensi-

tizer for the cavitation-induced radical formation, due to the weak O–O bond. The present study is a good example of how cavitation can be of synthetic value. This is complementary to the widely-used destructive approach, e.g. in the abatement of pollutants in waste-water treatment.

References

- [1] (a) J.H. Bang, K.S. Suslick, *J. Am. Chem. Soc.* 129 (2007) 2242; (b) S.-X. Wang, J.-T. Li, W.-Z. Yang, T.-S. Li, *Ultrasonics Sonochemistry* 9 (2002) 159; (c) C. Deng, H. Hu, X. Ge, C. Han, D. Zhao, G. Shao, *Ultrasonics Sonochemistry* 18 (2011) 932.
- [2] J. Huang, Y. Liu, Z. Song, Q. Jin, Y. Liu, X. Wang, *Ultrasonics Sonochemistry* 17 (2010) 521.
- [3] H. Xia, Q. Wang, Y. Liao, X. Xu, S.M. Baxter, R.V. Slone, S. Wu, G. Swift, D.G. Westmoreland, *Ultrasonics Sonochemistry* 9 (2002) 152.
- [4] D.T.C. Yang, C.J. Zhang, P.P. Fu, G.W. Kabalka, *Synth. Commun.* 27 (1997) 1601.
- [5] (a) J.-L. Luche, *Ultrasonics Sonochemistry* 1 (1994) S111.; (b) B.S. Bhatkhande, S.D. Samant, *Ultrasonics Sonochemistry* 5 (1998) 7; (c) M.-L. Wang, V. Rajendran, *Ultrasonics Sonochemistry* 14 (2007) 368.
- [6] (a) P. Riesz, D. Berdahl, C.L. Christman, *Env. Health Persp.* 64 (1985) 233; (b) K.S. Suslick, *Sonocatalysis*, in: G. Ertl, H. Knözinger, F. Schüth, J. Weitkamp (Eds.), *Handbook of Heterogeneous Catalysis*, second ed., Wiley-VCH, Weinheim, 2008.
- [7] (a) I. Hua, M.R. Hoffmann, *Environ. Sci. Technol.* 31 (1997) 2237; (b) T.J. Mason, *Adv. Sonochem.* 6 (2001) 247; (c) N.M. Mahamuni, Y.G. Adewuyi, *Ultrasonics Sonochemistry* 17 (2010) 990.
- [8] J.-L. Luche, *Synthetic Organic Sonochemistry*, Plenum Press, New York, 1998.
- [9] (a) G.J. Prize, D.J. Norris, P.J. West, *Macromolecules* 25 (1992) 6447; (b) M.W.A. Kuijpers, D. van Eck, M.F. Kemmere, J.T.F. Keurentjes, *Science* 298 (2002) 1969; (c) G.J. Prize, *Ultrasonics Sonochemistry* 10 (2003) 277.
- [10] E. Nakamura, D. Machii, T. Inubushi, *J. Am. Chem. Soc.* 111 (1989) 6850.
- [11] T.P. Caulier, M. Maeck, J. Reisse, *J. Org. Chem.* 60 (1995) 272.
- [12] K.S. Suslick, P.F. Schubert, J.W. Goodale, *J. Am. Chem. Soc.* 103 (1981) 7342.
- [13] K.A. Chervinsky, V.N. Mal'tsev, *Ukr. Chim. J.* 32 (1966) 69.
- [14] E.M. Mokry, V.L. Starchevsky, *Adv. Sonochem.* 3 (1993) 257.
- [15] T.J. Mason, *Chem. Soc. Rev.* 26 (1997) 443.
- [16] L.A. Crum, J.B. Fowlkes, *Nature* 319 (1986) 52.
- [17] U.A. Peuker, U. Hoffmann, U. Wietelmann, S. Bandelin, R. Jung, *Sonochemistry*, in *Ullmann's Encyclopedia of Industrial Chemistry*, Wiley-VCH, Weinheim, 2006.
- [18] T.G. Leighton, *Ultrasonics Sonochemistry* 2 (1995) S123.
- [19] K.S. Suslick, *Science* 247 (1990) 1439.
- [20] V. Misik, P. Riesz, *Ultrasonics Sonochemistry* 3 (1996) S173.
- [21] (a) G. Franz, R.A. Sheldon, *Oxidation*, in *Ullmann's Encyclopedia of Industrial Chemistry*, Wiley-VCH, Weinheim, 2005; (b) U. Neuenschwander, N. Turrà, C. Aellig, P. Mania, I. Hermans, *Chimia* 64 (2010) 225.
- [22] I. Hermans, P.A. Jacobs, J. Peeters, *J. Mol. Cat. A* 251 (2006) 221.
- [23] (a) I. Hermans, P.A. Jacobs, J. Peeters, *Chem. Eur. J.* 12 (2006) 4229; (b) I. Hermans, P.A. Jacobs, J. Peeters, *Chem. Eur. J.* 13 (2007) 754.
- [24] U. Neuenschwander, F. Guignard, I. Hermans, *ChemSusChem* 3 (2010) 75.
- [25] K.-G. Fahlbusch, F.-J. Hammerschmidt, J. Panten, W. Pickenhagen, D. Schatkowski, *Flavors and Fragrances*, in *Ullmann's Encyclopedia of Industrial Chemistry*, Wiley-VCH, Weinheim, 2005.
- [26] U. Neuenschwander, E. Meier, I. Hermans, *ChemSusChem* 4 (2011) 1613.
- [27] W. Riemenschneider, *Carboxylic Acids*, in *Ullmann's Encyclopedia of Industrial Chemistry*, Wiley-VCH, Weinheim, 2012.
- [28] (a) G.E. Zaikov, J.A. Howard, K.U. Ingold, *Can. J. Chem.* 47 (1969) 3017; (b) J.R. McNesby, C.A. Heller, *Chem. Rev.* 54 (1954) 325.
- [29] C. Kohlpaintner, M. Schulte, J. Falbe, P. Lappe, J. Weber, *Aldehydes*, in *Ullmann's Encyclopedia of Industrial Chemistry*, Wiley-VCH, Weinheim, 2012.
- [30] D.G. Truhlar, B.C. Garrett, *J. Phys. Chem.* 100 (1996) 12771.
- [31] N.N. Mahamuni, A.B. Pandit, *Ultrasonics Sonochemistry* 13 (2006) 165.
- [32] H. Fiege, *Cresols and Xylenols*, in *Ullmann's Encyclopedia of Industrial Chemistry*, Wiley-VCH, Weinheim, 2012.
- [33] U. Neuenschwander, I. Hermans, *J. Catal.* 287 (2012) 1.
- [34] G.H. Williams, *Advances in Free Radical Chemistry*, Elek, London, 1972.
- [35] H. Klenk, P.H. Götz, R. Siegmeyer, W. Mayr, *Peroxy Compounds*, *Organic*, in *Ullmann's Encyclopedia of Industrial Chemistry*, Wiley-VCH, Weinheim, 2012.
- [36] V. Misik, P. Riesz, *Ultrasonics Sonochemistry* 3 (1996) 25.